Delocalization-localization transition of plasmons in random $(GaAs)_m(Al_{0.3}Ga_{0.7}As)_6$ superlattices

Yu. A. Pusep,[1] A. D. Rodrigues,[1] and S. S. Sokolov[2]
[1]*Instituto de Fisica de São Carlos, Universidade de São Paulo, 13560-970 São Carlos, SP, Brazil*
[2]*B. Verkin Institute for Low-Temperature Physics and Engineering, National Academy of Sciences of Ukraine, 61164 Kharkov, Ukraine*
(Received 27 July 2009; revised manuscript received 25 September 2009; published 9 November 2009)

The transition of plasmons from propagating to localized state was studied in disordered systems formed in GaAs/AlGaAs superlattices by impurities and by artificial random potential. Both the localization length and the linewidth of plasmons were measured by Raman scattering. The vanishing dependence of the plasmon linewidth on the disorder strength was shown to be a manifestation of the strong plasmon localization. The theoretical approach based on representation of the plasmon wave function in a Gaussian form well accounted for by the obtained experimental data.

DOI: 10.1103/PhysRevB.80.205307 PACS number(s): 71.45.Gm, 71.55.Jv, 72.15.Rn

I. INTRODUCTION

As it was pointed out in Ref. 1, the problem of localization is fundamentally attributed to the wave nature of elementary excitations and therefore, may be equally studied by examination of properties of single-particle or collective excitations. Moreover, the probe of localization by Raman scattering of plasmons is even more desirable because it represents a direct measure of their wave functions (one-particle density of states), whereas conductivity measures two-electron properties. In our recent works[2,3] we investigated and compared the localization lengths of single-particle (electron) and collective (plasmon) excitations in disordered GaAs/AlGaAs superlattices (SLs), determined by means of quantum interference and Raman scattering, respectively. It was shown that the same random potential causes the localization of both plasmons and electrons and that plasmons are much stronger affected by disorder. However, only the weak localization regime was examined because of the complexity of the analysis of interference effects in the case of the strong localization. To the best of our knowledge the strong localization of any collective excitations was not yet studied. Therefore, the investigation of the strong plasmon localization may shed some light on the problem of the localization of collective excitations in general. An evident advantage of SLs is the quantitative control of the disorder strength managed by random variation in as-grown SL potential. Besides, a much bigger absolute value of the disorder strength may be achieved in SLs due to the large disorder scale as compared to the atomic size disorder caused by impurities. As demonstrated in this work, in order to achieve the strong plasmon localization the last statement is particularly essential. The random SL potential effectively localizes plasmons along the growth direction (perpendicular to the layers).[4] The theory sets up a direct connection between the intensity of Raman scattering and the plasmon wave function.[5] Therefore, Raman scattering presents the perfect tool to study the localization of the collective electron excitations. It ought to be also mentioned that understanding of physical principles of propagation and localization of plasmons is fundamentally important for development of ultrafast signal-processing nanophotonic devices, the research field currently experiencing an exponential growth.[6–10]

Contrary to electrical measurements where the localization of electrons may be simply detected, for instance, by the temperature dependence of conductivity, no such an evident criterion of the localization exists for plasmons. In order to detect the delocalization-localization transition, we analyzed the behavior of the plasmon linewidth (damping Γ_p) as a function of the disorder strength. We treat the delocalization regime, even though a plasmon excitation is described by a Gaussian-type wave function, as the limit where increasing disorder results in a corresponding increase in the linewidth broadening. In this limit $L_c \gg \Lambda$, where L_c is the localization scale of the Gaussian (the plasmon localization length) and Λ is the characteristic disorder length. On the contrary, the disorder does not affect the plasmon linewidth when $L_c \ll \Lambda$, which we interpret as strong localization of plasmon within the length Λ. The transition between these two regimes is attributed to the delocalization-localization transition.

II. EXPERIMENT

The spatial localization of collective excitations was achieved along the growth direction of the artificially disordered GaAs/AlGaAs SLs. The random $(GaAs)_m(Al_{0.3}Ga_{0.7}As)_6$ SLs, where the thicknesses of the layers are expressed in monolayers (MLs), with random variation in m around the nominal value 17 ML, were grown by molecular-beam epitaxy on semi-insulating (001) GaAs substrates. The disorder was characterized by the parameter $\delta=\Delta/W$, where Δ and $W=52$ meV are the width of the Gaussian distribution of the single-electron energies and the width of the miniband in the nominally periodic SL (calculated by the envelope function approximation). Due to the monolayer fluctuations $\delta=0.18$ even in the nominally periodic SL. The samples were homogeneously doped with Si to obtain equal electron concentrations $n=1.2\times10^{18}$ cm^{-3}. In addition, the nominally periodic $(GaAs)_{17}(AlAs)_2$ SLs with different electron densities in the range $(0.7–2.5)\times10^{18}$ cm^{-3} were investigated; in this case the disorder is produced by random impurity distribution while the disorder strength is proportional by impurity concentration. The damping and the spatial extents L_c of the plasmonlike coupled modes propagated along the growth direction (z) were measured at $T=10$ K by Raman back scattering in

$z(xy)\bar{z}$ configuration (where z is the direction perpendicular to the sample surface), when the longitudinal optical (LO) vibrations are active. They were associated with the dampings and the spatial localization lengths of the collective excitations subject to the superlattice or impurity disorder.

As will be explained below, two different regimes of the plasmon localization were achieved: (i) the regime of the weak localization in the periodic differently doped SLs and (ii) the regime of the strong localization in the intentionally disordered SLs with a fixed doping. The homogeneous distribution of the impurities over the doped SLs causes the isotropic plasmon localization within the wells. Therefore, in order to determine the dampings and the localization lengths of the plasmons in the periodic doped SLs we used the simple model of the spherical well localization potential.[11] While, in the case of the strong localization the plasmons were found overdamped ($\Gamma_p \gtrsim \omega_p$, where ω_p is the plasmon frequency). In such case the Raman intensity calculated in Refs. 12–14 were used to fit a corresponding Raman line and to determine the plasmon damping.

III. THEORETICAL CONSIDERATIONS

In the following we present the calculation of the plasmon linewidth $\Gamma_p = \hbar/\tau_p$, where τ_p is the plasmon lifetime, as a function of disorder. Herewith the limit of weak scattering is considered which, as will be shown later, indicates proper behavior of the plasmon damping even in the localization limit. The choice of the plasmon wave function is the crucial point of the problem. In Ref. 15 different approaches to a confined wave function of the longitudinal optical phonons. It was shown that the best approach is given by a Gaussian form of the wave function. Therefore, in analogy with the longitudinal optical phonons we suggest the trial wave function of localized plasmon as

$$\Psi_1(r) = \frac{2\sqrt{2}}{\pi^{1/4} L_c^{3/2}} \exp\left(-\frac{2r^2}{L_c^2}\right), \tag{1}$$

where L_c is calculated within variational ansatz for Hamiltonian containing potential energy given by the interaction with ionized impurities. As a matter of fact, in our approach L_c represents a measure of a correlated electron motion: the increasing disorder breaks down the correlation between the electrons destroying the plasmon that results in decreasing localization length. The quantum-mechanical definition for the linewidth of a single discrete state $|1\rangle$ associated with the plasmon is

$$\tau_p^{-1} = \frac{2\pi}{\hbar} |\langle 1|U|1\rangle|^2 \rho(E_p), \tag{2}$$

where E_p and $\rho(E_p)$ are the energy and the density of states of the plasmon. Here U is the perturbation potential taken in the form of neutral impurity potential $U = U_0 \theta(R_0 - r)$ with U_0 and R_0 being the amplitude of the scattering potential and the characteristic impurity size, respectively. To estimate τ_p, we suppose, in a spirit of self-consistent Born approximation, the Gaussian-type plasmon density of states, which in our case of a single state is

$$\rho(E_p) = \sqrt{\frac{2}{\pi}} \frac{\tau_p}{\hbar}. \tag{3}$$

Calculating the matrix element $|\langle 1|U|1\rangle|$ by the wave function of Eq. (1) we obtain

$$|\langle 1|U|1\rangle| = U_0 F\left(\frac{2R_0}{L_c}\right) \tag{4}$$

with $F(x) = \mathrm{erf}(x) - \frac{2}{\sqrt{\pi}} x \exp(-x^2)$. Combining Eqs. (1)–(4) leads to the linewidth Γ_p as a function of the localization length,

$$\Gamma_p = (8\pi)^{1/4} U_0 F\left(\frac{2R_0}{L_c}\right). \tag{5}$$

Both the linewidth and the localization length of the plasmon were determined by Raman scattering in differently disordered SLs as functions of the disorder strength parameter δ. Thus, the behavior of the plasmon linewidth was examined as a function of the disorder strength.

IV. RESULTS AND DISCUSSION

The selected Raman spectra of the regular periodic SLs with different doping levels and of the intentionally disordered SLs are shown in Figs. 1(a) and 1(b), respectively. In the used back-scattering $z(xy)\bar{z}$ configuration the Raman response is caused by the collective modes propagated parallel to the growth direction. These modes are straightforwardly influenced by the SL potential and consequently, by the as-grown disorder. Three coupled plasmon-LO phonon modes are clearly distinguished in the nominally periodic SL ($\delta = 0.18$) shown in Fig. 1(b): the GaAs-like low-frequency mode ν^-, the mixed ν_1^+ mode, and the high-frequency AlAs-like plasmonlike ν_2^+ mode. The arrows show the positions of the GaAs-like and AlAs-like transverse optical phonons TO_1 and TO_2, respectively. In addition, the unscreened LO phonon of GaAs was observed at 292 cm^{-1} due to the surface depletion layer. The plasmonlike mode reveals the upward asymmetry which emerges due to the nonconservation of the quasimomentum in disordered systems. In such case the analysis of the line shape allows for determination of both the damping and the localization length of the plasmonlike mode.[2,3]

The behavior of the plasmonlike mode measured in the periodic $(GaAs)_{17}(AlAs)_2$ SLs with different electron concentrations is illustrated in Fig. 1(a). With increasing electron concentration the asymmetry (responsible for the localization length) and the broadening (responsible for the linewidth) of the Raman line associated with this mode increase. The linewidth and the localization length extracted by the fit of the line shape of this Raman line in differently doped periodic SLs are collected in Figs. 2(a) and 2(b). The dependence of the localization length on the disorder strength obtained by interpolation of the experimental data [shown by solid line in Fig. 2(b)] was used in the calculation of the plasmon linewidth according to Eq. (5). The plasmon linewidth calculated in this way with $R_0 = 0.25$ nm and $U_0 = 0.6$ eV agrees well with the experimental data. The atomic scale magnitudes of

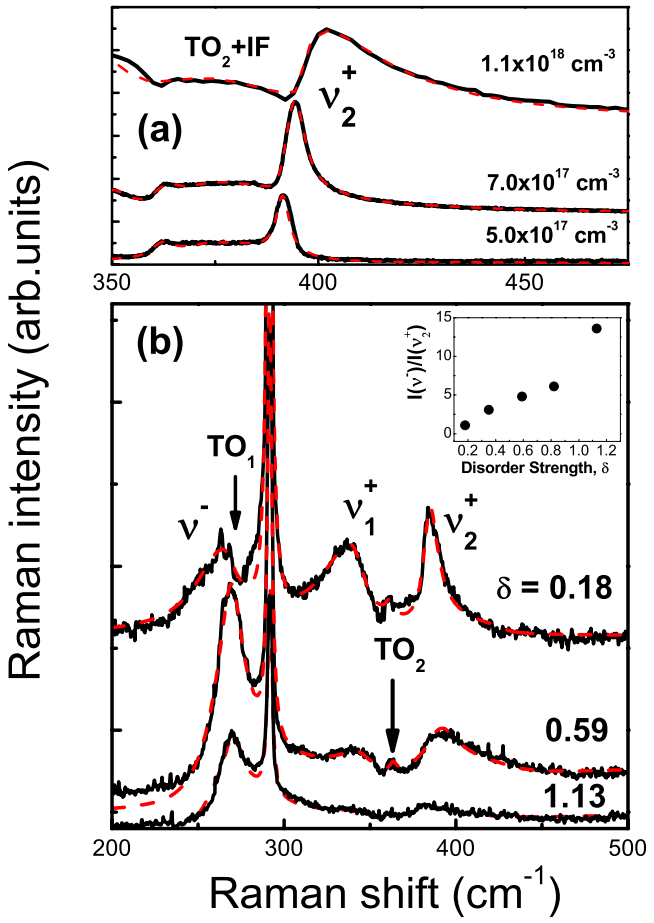

FIG. 1. (Color online) (a) Raman spectra measured in the range of the ν_2^+ coupled mode in differently doped $(GaAs)_{17}(AlAs)_2$ superlattices. (b) Raman spectra measured at $T=10$ K in the $(GaAs)_m(Al_{0.3}Ga_{0.7}As)_6$ superlattices with the electron density $n=1.2\times10^{18}$ cm^{-3} and different disorder strengths. The Raman intensities calculated as explained in the text are shown by the dark gray (red online) dashed lines. The spectra are vertically offset for clarity. The inset shows the ratio of the ν^- to ν_2^+ modes intensities measured in random superlattices.

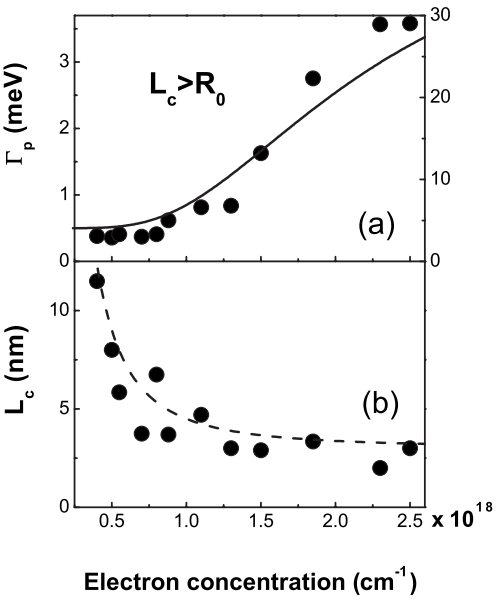

FIG. 2. Dampings of the (a) plasmonlike coupled ν_2^+ modes and (b) their localization length obtained in differently doped $(GaAs)_{17}(AlAs)_2$ superlattices. The line in (a) was calculated by Eq. (5) while the line in (b) was obtained by the interpolation procedure as explained in the text.

the size and the potential of impurity obtained by the fits imply that the plasmon broadening is due to the inelastic scattering by impurity (Si) core. This is in accord with the conclusion of Ref. 16 that in heavily doped semiconductors the main contribution to the plasmon localization comes from the interaction with the Coulomb potential of ionized impurities while the interaction with the impurity core (treated as the scattering by neutral impurities) does not significantly affect the plasmon localization length and may be considered as a perturbation influencing the plasmon linewidth. In this case the condition $R_0 \ll L_c$ indicates that the impurity scattering does not succeed strongly localize plasmons: the plasmons coherently determined within the space limited by L_c continue be propagating. As expected, in the limit of weak localization the increasing temperature decreases the localization length [shown in inset of Fig. 2(b)].

As was demonstrated in Ref. 3, in random SLs a strong enough intentional disorder dominates the impurity disorder even at relatively high electron concentration $(1-2)\times10^{18}$ cm^{-3}. The Raman spectra of some intentionally disordered SLs are depicted in Fig. 1(b). The effect of the quasimomentum nonconservation is evident in the corresponding asymmetries of all the coupled modes in the SL with the smallest disorder strength ($\delta=0.18$): according to their dispersions the ν^- and ν_1^+ modes reveal the downward asymmetries while the ν_2^+ mode shows the upward asymmetry. However, with increasing disorder strength the ν^- mode acquires the opposite upward asymmetry. In this case the plasmon damping produced by the random superlattice potential becomes so high that it results in the overdamped plasmon modes (when $\Gamma_p \gtrsim \omega_p$, where ω_p is the plasmon frequency). The characteristic features of the overdamped plasmon are the pining of the coupled plasmon-LO phonon modes at the frequency of the TO phonon and the upward Raman line asymmetry.[12–14] Both these features characterize the ν^- Raman lines observed at the TO_1 frequency in the random SLs with $\delta>0.3$ shown in Fig. 1(b). In such case the effect of the $q=0$ overdamped plasmons localized in the wells dominates the effect of the quasimomentum nonconservation and therefore, the plasmon damping was determined by the fit of the corresponding Raman line intensity calculated according to Ref. 14 to the experimental Raman line shape. At the same time as the high-frequency ν_2^+ mode remains to be determined by a relaxation of the q-vector selection rules in all the random SLs. Therefore, the localization lengths of the plasmonlike modes were obtained as in the doped SLs in the way described above. The results of the fits are shown in Fig. 1(b) by the dark gray (red online) dashed lines. The acquired plasmon dampings Γ_p are shown in Fig. 3(a). With the increasing disorder strength Γ_p exhibits a behavior different of that one observed in the doped periodic SLs: at a certain disorder ($\delta \gtrsim 0.4$) the plasmon damping ceases to reveal any

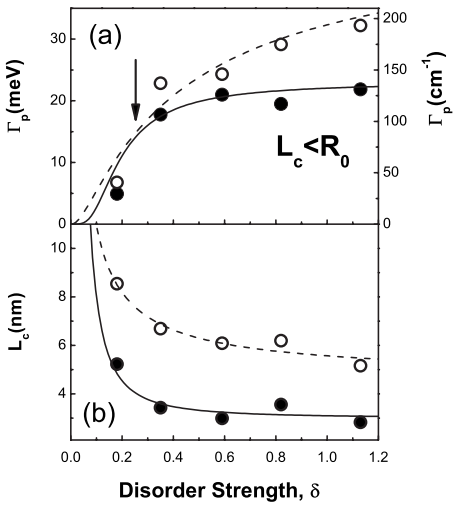

FIG. 3. (a) Linewidths Γ_p and (b) localization length L_c of plasmons obtained at the temperatures $T=10$ and 250 K (closed and open circles, respectively) in the $(GaAs)_m(Al_{0.3}Ga_{0.7}As)_6$ superlattices as functions of the disorder strengths. The lines in (a) were calculated by Eq. (5) with the dependencies $L_c(\delta)$, shown by the lines in (b), obtained by the interpolation procedure as explained in the text. The arrow in (a) separates the ranges corresponding to the propagating and localized plasmons.

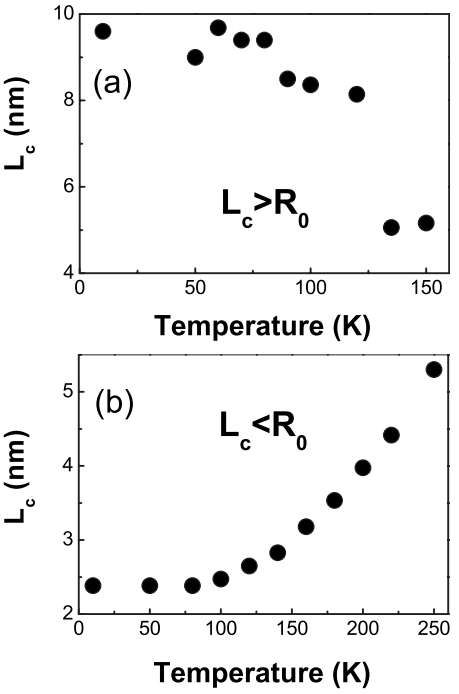

FIG. 4. The plasmon localization lengths measured (a) in the periodic superlattice with $n=2.5\times10^{18}$ cm^{-3} and (b) in the random superlattice with $\delta=1.13$ as a function of the temperature.

dependence on the disorder strength. Presumably, this behavior is caused by the strong localization of plasmons due to the superlattice disorder. In order to examine the effect of the localization on the plasmon linewidth we employed Eq. (5). Though our approach is valid for weak perturbations, Eq. (5) is applicable for any ratio $2R_0/L_c$. Consequently, a qualitatively correct behavior of the linewidth Γ_p as a function of the localization length L_c and/or the disorder strength δ is expected. Namely, Eq. (5) predicts the linewidth independent of the disorder strength at $L_c<R_0$. In such case R_0 may be attributed to the range within that plasmon is localized, i.e., $R_0\simeq\Lambda$. As shown in Fig. 3(b), the obtained decreasing plasmon localization length demonstrates the raise of localization with the increasing strength of the superlattice disorder potential. Again, the interpolated dependence of the localization length on the disorder strength was used in Eq. (5) to calculate the plasmon linewidth. The plasmon linewidth calculated in this way as a function of the disorder strength was found in good agreement with the experimental data. The best fit was obtained with $R_0=20.0$ nm and $U_0=15$ meV, which are close to the corresponding characteristic features of the random SL potential. As follows from the data shown in Fig. 3 in this case $R_0\approx L_c$ which corresponds to the strong localization limit. Moreover, the substantial increase in the integral intensity of the overdamped plasmon Raman line, located in the range of the GaAs lattice vibrations, relative to the intensity of the ν_2^+ plasmonlike line in the AlAs range was found with the increasing disorder strength [shown in inset of Fig. 1(b)]. This points out to the tendency of plasmons to localize in random GaAs wells, which proves the plasmon localization in the scale of the superlattice disorder demonstrated by the above analysis. It ought to be mentioned that the strong localization of the plasmons was achieved in the disordered SLs due to the substantial increase in the effective impurity size R_0, which in this case is determined by the well thicknesses. Thus, the regimes of the weak and strong plasmon localizations shown in Figs. 2 and 3 were distinguished at $L_c>R_0$ and $L_c\leq R_0$, respectively.

Furthermore, as any localized quasiparticles, plasmons can be delocalized when increasing the temperature. The corresponding data obtained at $T=250$ K are shown in Fig. 3 by open circles. The dependence of the plasmon damping on the disorder strength becomes smoother [similar to that one observed in the doped SLs in Fig. 2(a)] indicating the plasmon delocalization. In such case the theory gives $R_0=20.0$ nm and $U_0=60$ meV. Consequently the increasing temperature results in plasmon delocalization and effectively enhances the scattering potential. The different temperature variations in the localization lengths measured in the regimes of the weak and strong localizations, shown in Figs. 4(a) and 4(b), respectively, also exhibit the expected behavior. The plasmon localization length was found decreasing with the increasing temperature in the regime of the weak plasmon localization [Fig. 4(a)]. While, the plasmon localization increased with the increasing temperature in the regime of the strong plasmon localization [Fig. 4(b)]. These data were found consistent with the significantly weaker temperature decrease in the electron dephasing length (which serves as the lower cutoff for the electron localization length) observed in the regime of the strong localization as compared to the regime of the weak localization in Ref. 17. Thus, both the electrons and the plasmons demonstrate the same tendencies when increasing the disorder. In weakly disordered samples the localization length of the electrons and the plasmons decreases with the increasing temperature. The increasing disorder significantly weakens the temperature decrease in the electron localization

length, whereas this results in the opposite temperature behavior of the plasmon localization length. Consequently, a certain association of the localization of plasmons with the localization of electrons may be established.

V. CONCLUSION

In conclusion, the delocalization-localization transition of plasmons, analogous to the metal-to-insulator transition of electrons was demonstrated. The considerable influence of the disorder on the plasmon linewidth was detected for weak plasmon perturbation ($L_c > R_0$), which is the case of the doped periodic SLs reported here, where the inelastic scattering of plasmons by impurity cores is weak. While, the insignificant effect of the disorder on the plasmon linewidth was found in the random SLs where a strong disorder causes the plasmon localization within the length $L_c \leq R_0$. The independence of the plasmon damping on the disorder is considered as a manifestation of the strong plasmon localization. As expected, the increasing temperature enhances the localization of the weakly localized plasmons while it causes the delocalization of the strongly localized plasmons. In spite of the crudeness of the assumptions involved in our analysis, the present model is able to reproduce essential experimental features including the localization of plasmon in the scale of the disorder superlattice potential.

ACKNOWLEDGMENTS

Financial supports from Brazilian agencies FAPESP and CNPq are gratefully acknowledged.

[1] S. Das Sarma, A. Kobayashi, and R. E. Prange, Phys. Rev. Lett. **56**, 1280 (1986); Phys. Rev. B **34**, 5309 (1986).
[2] Y. A. Pusep, M. B. Ribeiro, V. E. Carrasco, G. Zanelatto, and J. C. Galzerani, Phys. Rev. Lett. **94**, 136407 (2005).
[3] Y. A. Pusep and A. Rodriguez, Phys. Rev. B **75**, 235310 (2007).
[4] Y. A. Pusep, M. T. O. Silva, J. C. Galzerani, N. T. Moshegov, and P. Basmaji, Phys. Rev. B **58**, 10683 (1998).
[5] R. Merlin, in *Light Scattering in Solids V*, edited by M. Cardona and G. Güntherodt (Springer-Verlag, Heidelberg, 1989).
[6] W. L. Barnes, A. Dereux, and T. W. Ebbesen, Nature (London) **424**, 824 (2003).
[7] S. A. Maier and H. A. Atwater, J. Appl. Phys. **98**, 011101 (2005).
[8] S. Grésillon, L. Aigouy, A. C. Boccara, J. C. Rivoal, X. Quelin, C. Desmarest, P. Gadenne, V. A. Shubin, A. K. Sarychev, and V. M. Shalaev, Phys. Rev. Lett. **82**, 4520 (1999).
[9] D. Pacifici, H. J. Lezec, and H. A. Arwater, Nat. Photonics **1**, 402 (2007).
[10] B. Fluegel, A. Mascarenhas, D. W. Snoke, L. N. Pfeiffer, and K. West, Nat. Photonics **1**, 701 (2007).
[11] H. Richter, Z. P. Wang, and L. Ley, Solid State Commun. **39**, 625 (1981).
[12] D. T. Hon and W. L. Faust, Appl. Phys. (Berlin) **1**, 241 (1973).
[13] G. Irmer, M. Wenzel, and J. Monecke, Phys. Rev. B **56**, 9524 (1997).
[14] A. Mlayah, R. Carles, G. Landa, E. Bedel, and A. Muños-Yagüe, J. Appl. Phys. **69**, 4064 (1991).
[15] I. H. Campbell and P. M. Fauchet, Solid State Commun. **58**, 739 (1986).
[16] Y. A. Pusep, S. S. Sokolov, W. Fortunato, J. C. Galzerani, and J. R. Leite, J. Phys.: Condens. Matter **13**, 10165 (2001).
[17] Y. A. Pusep, H. Arakaki, and C. A. de Souza, Phys. Rev. B **68**, 205321 (2003).